PHYSICAL REVIEW E **74**, 066206 (2006)

Chaotic dynamics and synchronization in microchip solid-state lasers with optoelectronic feedback

Atsushi Uchida, Keisuke Mizumura, and Shigeru Yoshimori
Department of Electronics and Computer Systems, Takushoku University, 815-1 Tatemachi, Hachioji, Tokyo 193-0985, Japan
(Received 13 July 2006; published 22 December 2006)

We experimentally observe the dynamics of a two-mode Nd:YVO_4 microchip solid-state laser with optoelectronic feedback. The total laser output is detected and fed back to the injection current of the laser diode for pumping. Chaotic oscillations are observed in the microchip laser with optoelectronic self-feedback. We also observe the dynamics of two microchip lasers coupled mutually with optoelectronic link. The output of one laser is detected by a photodiode and the electronic signal converted from the laser output is sent to the pumping of the other laser. Chaotic fluctuation of the laser output is observed when the relaxation oscillation frequency is close to each other between the two microchip lasers. Synchronization of periodic wave form is also obtained when the microchip lasers have a single-longitudinal mode.

DOI: 10.1103/PhysRevE.74.066206 PACS number(s): 05.45.Xt, 05.45.−a, 42.65.Sf

I. INTRODUCTION

Chaotic dynamics and synchronization behavior have been investigated in many laser systems for understanding universal laws in nonlinear dynamical systems, as well as for its potential applications to optical secure communications and spread spectrum communications. A variety of temporal and spatial dynamics with high dimensionality can be generated in lasers with time-delayed feedback [1,2]. Lasers with delayed optical feedback have been found to generate chaotic oscillations [3–5], however, these systems are sensitive to optical phase variations when the feedback optical field is coherent with optical field inside the laser cavity. Compared with optical feedback, optoelectronic feedback is reliable and robust because the system is insensitive to optical phase variations [6–8]. Chaos in a semiconductor laser with optoelectronic feedback to the injection current has been reported and quasiperiodic route to chaos has been observed [6]. Chaotic dynamics has been reported in a CO_2 gas laser with optoelectronic feedback to an intracavity electro-optic modulator (EOM) [9,10]. Synchronization of chaos has also been observed in one-way and mutually coupled semiconductor lasers with optoelectronic link [11,12] and in a CO_2 gas laser with optoelectronic feedback [13]. The use of cross-coupled semiconductor lasers with optoelectronic link has been pointed out for the prediction of the system dynamics of epidemics [14].

Although the optoelectronic feedback method has been applied to semiconductor lasers and gas lasers for generating chaos, there have been few reports on solid-state lasers with optoelectronic feedback. Solid-state lasers that have a short cavity length (typically less than one millimeter) are called microchip lasers. Due to their short cavity length, lasing occurs in a few longitudinal modes. Compared with other lasers, microchip lasers inherently have strong sustained relaxation oscillation due to the quantum noise in a laser cavity, which may be crucial for the dynamics of microchip lasers. Although the dynamics of microchip solid-state lasers have been investigated intensively [15–18], most studies have been focused on chaos induced by external modulation to the pumping laser or the cavity loss. A few studies on chaos has been reported in Nd:YAG microchip lasers with optoelectronic feedback to an intracavity acousto-optic modulator (AOM) [19–21]. In this case a time-delayed feedback signal modulates the loss of the laser cavity and induces chaotic instability. A sudden transition from steady state to high-amplitude chaotic spiking behavior has been observed [19].

In this study we investigate chaotic dynamics of a two-longitudinal-mode Nd:YVO_4 microchip solid-state laser with optoelectronic feedback to the injection current of the laser diode for pumping. The feedback signal directly affects the population inversion of the microchip laser, which is different from the systems in [19–21]. We change the relaxation oscillation frequency of the microchip laser and the feedback gain to observe bifurcation scenario. We also observe chaotic dynamics in two Nd:YVO_4 microchip lasers coupled mutually with optoelectronic link. Synchronization phenomenon is observed under single-longitudinal-mode operation.

II. ONE LASER WITH OPTOELECTRONIC FEEDBACK

A. Experimental setup

Figure 1 shows our experimental setup for the observation of chaotic dynamics in a microchip laser with optoelectronic feedback. We used a Nd:YVO_4 microchip crystal (1.1 atm % doped; II-VI Inc.), pumped by a laser diode (Coherent Inc., DCF81-1000C-100-FC) with two focusing lenses. The temperatures of the microchip crystal and the laser diode were controlled by thermoelectric coolers (resolution of 0.01 K) for fine tuning of the laser frequencies. The microchip laser oscillated with two-longitudinal modes at a wide range of pumping power, except near the lasing threshold. Although there are two relaxation oscillation frequencies for two-mode lasers, we focus on the fundamental (higher) relaxation oscillation frequency f_r for the main longitudinal mode in this paper. The output of the microchip laser was detected by a photodiode and converted to an electronic signal. The electronic signal was fed back to the injection current of the laser diode for pumping through a dc block (a high-pass filter with a cutoff frequency of 16 kHz), some attenuators (Stack Electronics Co. Ltd., BNC-PJ), and an

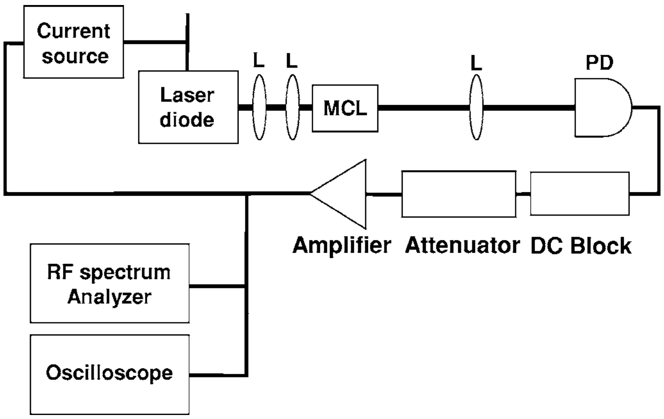

FIG. 1. Experimental setup of a microchip solid-state laser with optoelectronic feedback. L, lens; MCL, Nd:YVO_4 microchip solid-state laser; PD, photodiode. The thick and thin lines indicate laser beams and electronic coaxial cables, respectively.

electronic amplifier (NF Corporation, CA-251F4, bandwidth from dc to 10 MHz, gain of 40 dB). Coaxial attenuators were combined to change the attenuation ratio from −40 to −20 dB and the net gain of the whole feedback loop was changed from −4 to 16 dB. The feedback delay time was 0.25 μs, which was comparable with the inverse of the relaxation oscillation frequency f_r of the microchip laser (f_r =1–4 MHz, $1/f_r$=0.25–1.0 μs). Positive feedback without dc component was achieved. Chaotic temporal wave forms of the microchip laser was detected with the photodiode and a digital oscilloscope (Sony Tektronix, TDS420, 100 Mega samples/s). Radio-frequency (rf) spectrum of the microchip laser was measured with a rf spectrum analyzer (Advantest, R3131, bandwidth from 9 kHz to 3 GHz).

B. Experimental results

We fixed the net gain of the feedback loop of 7 dB and varied the relaxation oscillation frequency f_r by changing the injection current I of the laser diode for pumping. Note that f_r increases monotonously as I is increased. The lasing threshold of the microchip laser was I_{th}=269 mA without feedback. Figure 2 shows the temporal wave forms and the corresponding rf spectra at various relaxation oscillation frequencies. Slow switching behavior between nonlasing and steady lasing states is observed at frequencies of tens of Hz just above the laser threshold (not shown in Fig. 2), and sustained relaxation oscillation is observed at around f_r =2.00 MHz (I=360 mA). Period-1 oscillation is observed at f_r=2.22 MHz (I=380 mA) as shown in Figs. 2(a) and 2(b). As f_r is increased, coexisting states between period-1 and chaotic oscillations are observed at f_r=2.27 MHz (I =393 mA) as shown in Figs. 2(c) and 2(d). Chaotic oscillation appears from f_r=2.30 MHz to f_r=3.54 MHz (from I =398 mA to I=517 mA) as shown in Figs. 2(e) and 2(f). The fundamental frequency of the temporal wave forms is dominated by f_r and there exists a large peak of f_r in the rf spectrum. The transition from period-1 to chaos through their coexisting states is observed. We cannot find a clear bifurcation scenario to chaos such as period-doubling and quasiperiodic breakdown routes in this system.

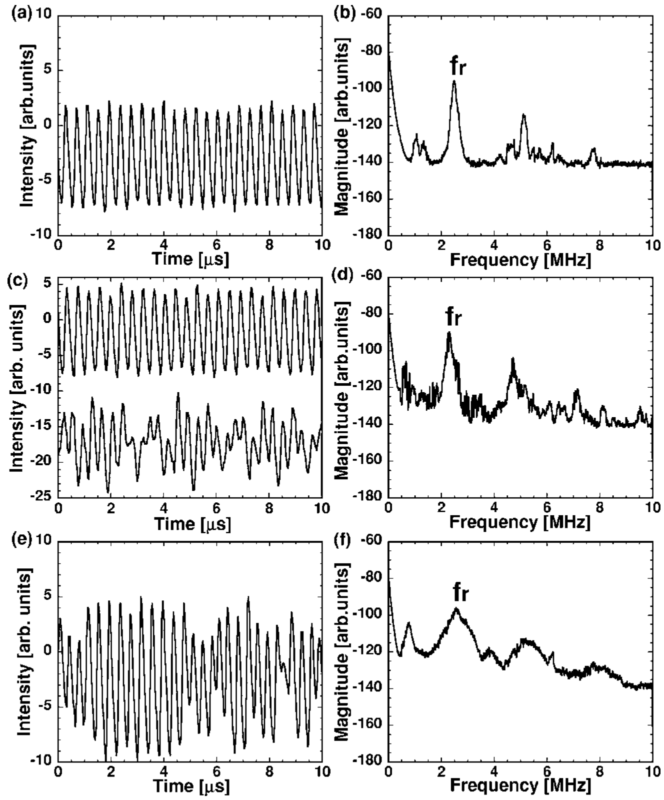

FIG. 2. Temporal wave forms and corresponding rf spectra of the microchip laser with optoelectronic feedback. (a), (b) f_r =2.22 MHz, (c), (d) f_r=2.27 MHz, (e), (f) f_r=2.56 MHz. The two temporal wave forms in (c) are obtained at different times, showing coexisting state between period-1 and chaotic oscillations. (a), (b) Period-1 oscillation, (c), (d) coexisting state, and (e), (f) chaotic oscillation.

We changed both the relaxation oscillation frequency f_r and the feedback gain G simultaneously and create a two-dimensional dynamical map. Figure 3 shows the dynamical map as functions of f_r and G. Below f_r=2.2 MHz, sustained

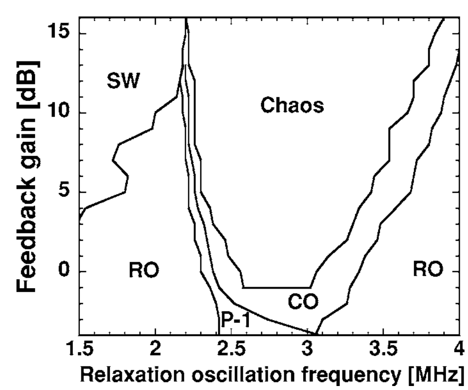

FIG. 3. Two-dimensional map of the microchip laser with optoelectronic feedback, as functions of the relaxation oscillation frequency and the feedback gain. SW, switching behavior; RO, sustained relaxation oscillation; P-1, period-1 oscillation; CO, coexisting state between period-1 and chaotic oscillations.

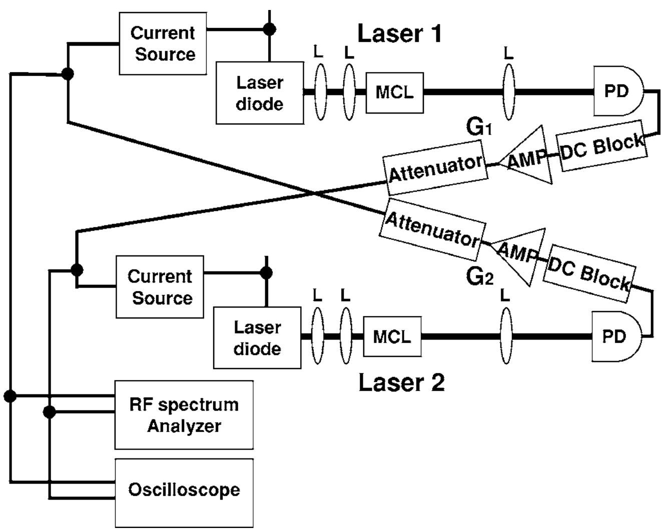

FIG. 4. Experimental setup for two microchip lasers coupled with optoelectronic link. AMP, electronic amplifier; L, lens; MCL, Nd:YVO_4 microchip solid-state laser; PD, photodiode. The thick and thin lines indicate laser beams and electronic coaxial cables, respectively.

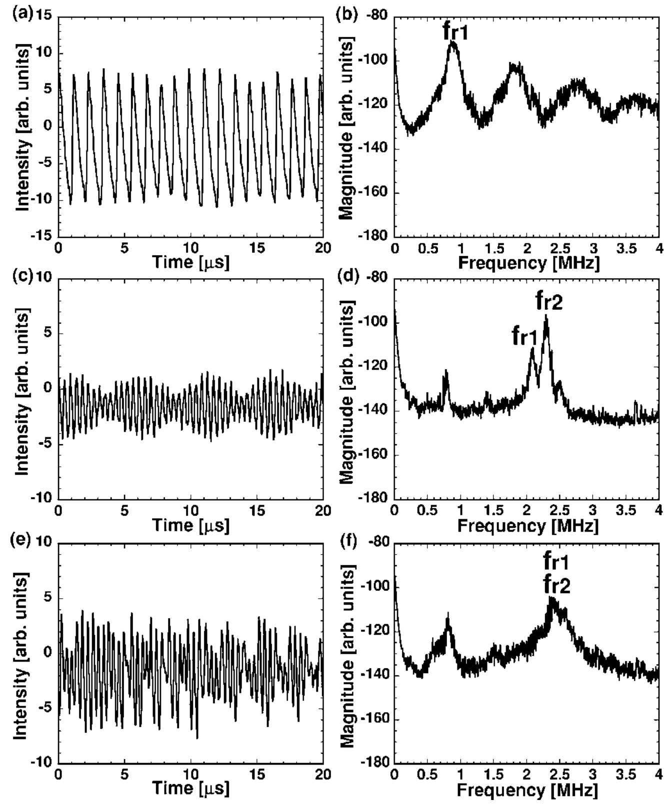

FIG. 5. Temporal wave forms and corresponding rf spectra of laser 1 with mutual optoelectronic coupling. (a), (b) $f_{r1}=0.85$ MHz; (c), (d) $f_{r1}=2.09$ MHz; and (e), (f) $f_{r1}=2.40$ MHz. (a), (b) Period-1 oscillation; (c), (d) quasiperiodic oscillation; and (e), (f) chaotic oscillation.

relaxation oscillation (RO) is observed at small G and slow switching behavior (SW) between nonlasing and steady lasing states appears at frequencies of tens of Hz at large G. At around $f_r=2.2$–2.5 MHz, the transition from period-1 (P-1) to chaos through their coexisting states (CO) is observed. Chaos can be observed at wide range of the parameter space. At $f_r>3.5$ MHz chaotic oscillation disappears and sustained relaxation oscillation is observed again, because the nonlinear interaction becomes weak between the two inherent frequencies: the relaxation oscillation frequency f_r and the inverse of the feedback delay time. The relaxation oscillation frequency at the chaotic region ($f_r=2.5$–3.5 MHz) closely corresponds to the inverse of the feedback delay time ($\tau=0.25$ μs) in the chaotic regime. The two frequency components must be close enough to generate chaotic oscillations.

III. TWO LASERS COUPLED WITH OPTOELECTRONIC LINK

A. Experimental setup

We investigate the dynamics of mutually coupled two microchip lasers with optoelectronic link. Figure 4 shows the experimental setup. The output of one Nd:YVO_4 microchip laser (laser 1) was detected by a photodiode and the converted electronic signal was sent to the injection current of the laser diode for pumping of the other Nd:YVO_4 microchip laser (laser 2) through a dc block, some attenuators, and an amplifier (the same components in the preceding section). The output of laser 2 was also detected with another photodiode and the electronic signal was sent to the injection current of the other laser diode for laser 1. Positive coupling without dc component was achieved. The cross coupling through optoelectronic link provided complex dynamical behavior. The lasing thresholds for lasers 1 and 2 without coupling were 269 and 272 mA, respectively.

B. Experimental results

We fixed the net coupling gains of $G_1=0$ and $G_2=8$ dB for lasers 1 and 2, respectively. The delay time from laser 1 to laser 2 was 0.26 μs, and the delay time from laser 2 to laser 1 was 0.25 μs. The relaxation oscillation frequency of laser 2 was set to $f_{r2}=2.32$ MHz ($I_2=367$ mA). We changed the relaxation oscillation frequency of laser 1 f_{r1} to observe the dynamics of the mutually coupled microchip lasers. Figure 5 shows the temporal wave forms and the corresponding rf spectra of laser 1 with mutual optoelectronic coupling. When f_{r1} is less than 0.66 MHz ($I_1<320$ mA), slow switching behavior between nonlasing and steady lasing states is observed (not shown in Fig. 5). The switching frequency is tens of Hz depending on the injection current. As f_{r1} is increased, period-1 oscillation is observed at around $f_{r1}=0.85$ MHz, as shown in Figs. 5(a) and 5(b). Sustained relaxation oscillation is also observed from $1.94<f_{r1}<2.02$ MHz ($367<I_1<374$ mA). Then quasiperiodic oscillation appears at around $f_{r1}=2.09$ MHz because of the interaction between the two relaxation oscillation frequencies of f_{r1} and f_{r2} for laser 1 and laser 2, as shown in Figs. 5(c) and 5(d). As f_{r1} approaches f_{r2}(=2.32 MHz), quasiperiodic oscil-

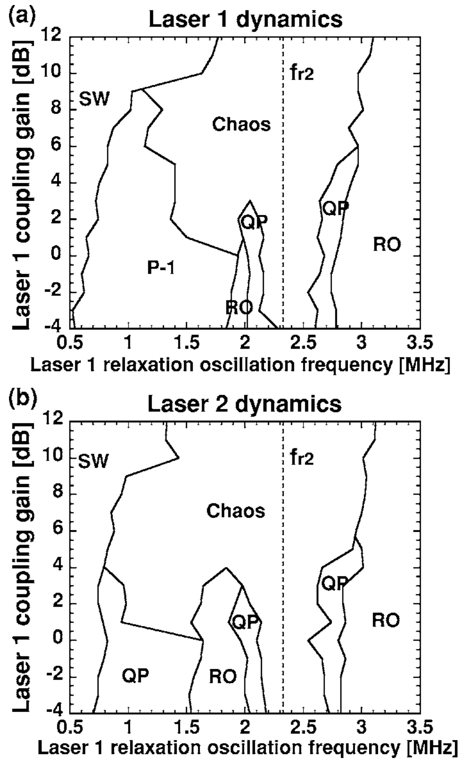

FIG. 6. Two-dimensional map of the two microchip lasers coupled with optoelectronic link for (a) laser 1 and (b) laser 2, as functions of the relaxation oscillation frequency of laser 1 (f_{r1}) and the coupling gain of laser 1 (G_1). The dotted line indicates the relaxation oscillation frequency of laser 2 (f_{r2}=2.32 MHz). SW, switching behavior; RO, sustained relaxation oscillation; P-1, period-1 oscillation; QP, quasiperiodic oscillation.

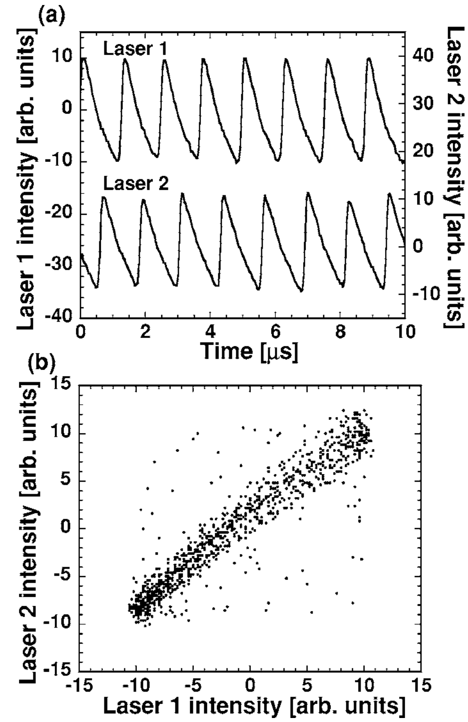

FIG. 7. (a) Temporal wave forms and (b) time-shifted correlation plot of two coupled microchip lasers. Synchronization of period-1 oscillation is observed. The cross correlation between the two temporal wave forms is 0.920.

lation breaks down and chaotic oscillation is observed at the range of $2.12 < f_{r1} < 2.68$ MHz ($380 < I_1 < 412$ mA), as shown in Figs. 5(e) and 5(f). The rf spectrum is broadened in the presence of chaos. Quasiperiodic oscillation is observed again when f_{r1} is further increased. Finally sustained relaxation oscillation appears at $f_{r1} > 2.78$ MHz ($I_1 > 416$ mA). Quasiperiodic breakdown scenario to chaos is observed in this mutually coupled microchip laser system, as well as gas lasers and semiconductor lasers with optoelectronic link reported in [10,12].

We next changed both f_{r1} and G_1 simultaneously and create two-dimensional dynamical maps for lasers 1 and 2. We fixed f_{r2}=2.32 MHz and G_2=8 dB. Figure 6 shows the two-dimensional maps of the dynamics of lasers 1 and 2 as functions of f_{r1} and G_1. Chaos is observed when f_{r1} is close to f_{r2}=2.32 MHz (the dotted line in Fig. 6) because of the nonlinear interaction between f_{r1} and f_{r2}. Quasiperiodic breakdown route to chaos is observed at small G_1, whereas a sudden transition to chaos appears at large G_1. Slow switching behavior becomes dominant at large G_1 and small f_{r1}. Note that the dynamics of lasers 1 and 2 are slightly different, where period-1 oscillation only appears for laser 1 at f_{r1} =0.5–1.8 MHz. This asymmetric behavior results from the mismatch of the lower relaxation oscillation frequency for the second longitudinal mode. We cannot match both the higher and lower relaxation oscillation frequencies between lasers 1 and 2 since the ratio between the two relaxation oscillation frequencies in a two-mode microchip laser is different for each laser device. Therefore, we cannot observe synchronization of either chaotic or periodic wave forms between the two microchip lasers in this two-mode configuration due to the mismatch of the two relaxation oscillation frequencies.

C. Synchronization of periodic wave forms

We investigate synchronization in the mutually coupled microchip lasers with optoelectronic link in detail. We decreased the injection current of the laser diodes for pumping and set it near the lasing threshold in order to achieve single-longitudinal-mode operation of the microchip lasers. The injection currents of the laser diodes for lasers 1 and 2 were set to I_1=326 mA ($1.21 I_{th,1}$) and I_2=320 mA ($1.18 I_{th,2}$), respectively. There existed one relaxation oscillation frequency for each single-mode microchip laser and the relaxation oscillation frequency was matched between lasers 1 and 2 (f_{r1} $=f_{r2}$=1.17 MHz). We set the net coupling gain of G_1 =−2 dB and G_2=0 dB. Figure 7 shows the temporal wave forms of the two microchip lasers and their correlation plot. The period-1 oscillations are synchronized to each other with time delay. The time-shifted cross correlation shown in Fig. 7(b) indicate synchronization of the periodic wave forms. The average delay time is 0.6 μs, corresponding to half-period of the temporal wave forms in Fig. 7(a). We cannot find leader-laggard relationship [22] between the two micro-

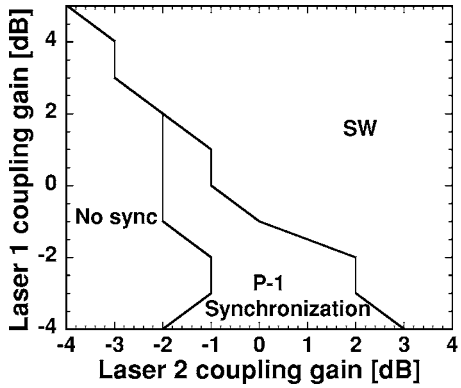

FIG. 8. Two-dimensional map of the two microchip lasers coupled with optoelectronic link at single-mode operation, as functions of coupling gains of laser 1 and laser 2 (G_1 and G_2). SW, switching behavior; *P*-1, synchronization; synchronization of period-1 wave forms; no sync, no synchronization.

chip lasers because we only obtain synchronization of periodic wave forms.

We changed two coupling gains G_1 and G_2 and investigated the synchronization region. We define synchronization when the cross correlation [20,21] between the two temporal wave forms is larger than 0.9. Figure 8 shows the synchronization map as functions of G_1 and G_2. We observe synchronization of period-1 wave forms at around $-2 < G_2 < 3$ dB and small G_1. In the region of $G_2 < -2$ dB, no synchronization is observed. In this region, periodic wave forms are observed in laser 1 and the coexisting states between period-1 and quasiperiodic wave forms are obtained in laser 2. As G_1 and G_2 are increased, slow switching behavior between nonlasing and steady lasing states is observed because of large coupling gain. The threshold for switching behavior is roughly estimated from the sum of G_1 and G_2, i.e., $G_1 + G_2 = -1 \sim 1$ dB.

We only observed synchronization of periodic wave forms, but not chaotic wave forms. We observed synchronization of slow frequency components of chaotic oscillations at frequencies of kHz, but not fast chaotic oscillations at frequencies of MHz. The coupling strength is not enough to induce good quality of chaos synchronization in our configuration. Since the two microchip lasers operate near the lasing threshold in order to maintain single-longitudinal-mode operation, the switching behavior easily appears at small coupling gain before synchronization of chaos is observed. We speculate that synchronization of chaos may occur when two single-mode microchip lasers with large pumping power are coupled with large coupling gain. Different types of coupling (positive or negative, and ac or dc) may also induce new chaotic dynamics and synchronization of chaos in microchip solid-state lasers with optoelectronic link.

IV. CONCLUSION

We have experimentally observed the dynamics of a two-longitudinal-mode $Nd:YVO_4$ microchip solid-state laser with optoelectronic feedback. Chaotic oscillations are observed in the microchip laser with optoelectronic self-feedback when the laser output is fed back to the injection current of the laser diode for pumping. We have also observed the dynamics of two microchip lasers coupled mutually with optoelectronic link to the other laser diode for pumping. Quasiperiodic breakdown scenario to chaos is found and chaotic fluctuation of the laser output is observed when the relaxation oscillation frequency is close to each other between the two microchip lasers. Synchronization of periodic wave form is also obtained under a single-longitudinal-mode operation in the two microchip lasers.

ACKNOWLEDGMENTS

The authors thank Riccardo Meucci, Junji Ohtsubo, Rajarshi Roy, and Ira B. Schwartz for helpful discussions. The authors gratefully acknowledge support from the Support Center for Advanced Telecommunications Technology Research and Grants-in-Aid for Scientific Research from the Japan Society for the Promotion of Science.

[1] R. Vicente, J. Daudén, P. Colet, and R. Toral, IEEE J. Quantum Electron. **41**, 541 (2005).
[2] A. Uchida, F. Rogister, J. García-Ojalvo, and R. Roy, Prog. Opt. **48**, 203 (2005).
[3] R. Lang and K. Kobayashi, IEEE J. Quantum Electron. **16**, 347 (1980).
[4] B. Tromborg, J. H. Osmundsen, and H. Olesen, IEEE J. Quantum Electron. **20**, 1023 (1984).
[5] I. Fischer, G. H. M. van Tartwijk, A. M. Levine, W. Elsäßer, E. Göbel, and D. Lenstra, Phys. Rev. Lett. **76**, 220 (1996).
[6] S. Tang and J. M. Liu, IEEE J. Quantum Electron. **37**, 329 (2001).
[7] F. Rogister, A. Locquet, D. Pieroux, M. Sciamanna, O. Deparis, P. Megret, and M. Blondel, Opt. Lett. **26**, 1486 (2001).
[8] J. M. Saucedo Solorio, D. W. Sukow, D. R. Hicks, and A. Gavrielides, Opt. Commun. **214**, 327 (2002).
[9] F. T. Arecchi, W. Gadomski, and R. Meucci, Phys. Rev. A **34**, 1617 (1986).
[10] F. T. Arecchi, G. Giacomelli, A. Lapucci, and R. Meucci, Phys. Rev. A **43**, 4997 (1991).
[11] S. Tang and J. M. Liu, Opt. Lett. **26**, 596 (2001).
[12] R. Vicente, S. Tang, J. Mulet, C. R. Mirasso, and J.-M. Liu, Phys. Rev. E **70**, 046216 (2004).
[13] E. Allaria, F. T. Arecchi, A. DiGarbo, and R. Meucci, Phys. Rev. Lett. **86**, 791 (2001).
[14] M. Y. Kim, R. Roy, J. L. Aron, T. W. Carr, and I. B. Schwartz, Phys. Rev. Lett. **94**, 088101 (2005).
[15] P. Mandel, *Theoretical Problems in Cavity Nonlinear Optics* (Cambridge University Press, Campridge, UK, 1997).
[16] K. Otsuka, *Nonlinear Dynamics in Optical Complex Systems* (KTK Scientific Publisher, Tokyo, 1999).
[17] K. Otsuka, IEEE J. Quantum Electron. **15**, 655 (1979).

[18] A. Uchida, T. Ogawa, M. Shinozuka, and F. Kannari, Phys. Rev. E **62**, 1960 (2000).
[19] R. Meucci, R. McAllister, and R. Roy, Phys. Rev. E **66**, 026216 (2002); R. McAllister, R. Meucci, D. DeShazer, and R. Roy, *ibid.* **67**, 015202(R) (2003).
[20] A. Uchida, R. McAllister, R. Meucci, and R. Roy, Phys. Rev. Lett. **91**, 174101 (2003); R. McAllister, A. Uchida, R. Meucci, and R. Roy, Physica D **195**, 244 (2004).
[21] A. Uchida, R. McAllister, and R. Roy, Phys. Rev. Lett. **93**, 244102 (2004).
[22] T. Heil, I. Fischer, W. Elsäßer, J. Mulet, and C. R. Mirasso, Phys. Rev. Lett. **86**, 795 (2001).